On the Multiple Functional Roles of the Active Site Histidine in Catalysis and Allosteric Regulation of *Escherichia coli* Glucosamine 6-Phosphate Deaminase†

Gabriela M. Montero-Morán,‡ Samuel Lara-González,‡ Laura I. Álvarez-Añorve,‡ Jacqueline A. Plumbridge,§ and Mario L. Calcagno*,‡

Departamento de Bioquímica, Laboratorio de Fisicoquímica y Diseño de Proteínas, Facultad de Medicina, Universidad Nacional Autónoma de México (UNAM), P. O. Box 70-159, Mexico City 04510, D.F., México, and Institut de Biologie Physico-Chimique (CNRS, UPR9073), 75005 Paris, France

Received March 22, 2001; Revised Manuscript Received June 20, 2001

ABSTRACT: The active site of glucosamine-6-phosphate deaminase (EC 3.5.99.6, formerly 5.3.1.10) from *Escherichia coli* was first characterized on the basis of the crystallographic structure of the enzyme bound to the competitive inhibitor 2-amino-2-deoxy-glucitol 6-phosphate. The structure corresponds to the R allosteric state of the enzyme; it shows the side-chain of His143 in close proximity to the O5 atom of the inhibitor. This arrangement suggests that His143 could have a role in the catalysis of the ring-opening step of glucosamine 6-phosphate whose α-anomer is the true substrate. The imidazole group of this active-site histidine contacts the carboxy groups from Glu148 and Asp141, via its Nδ1 atom [Oliva et al. (1995) *Structure* 3, 1323−1332]. These interactions change in the T state because the side chain of Glu148 moves toward the allosteric site, leaving at the active site the dyad Asp141-His143 [Horjales et al. (1999) *Structure 7*, 527−536]. In this research, a dual approach using site-directed mutagenesis and controlled chemical modification of histidine residues has been used to investigate the role of the active-site histidine. Our results support a multifunctional role of His143; in the forward reaction, it is involved in the catalysis of the ring-opening step of the substrate, glucosamine 6-P. In the reverse reaction, the substrate fructose 6-P binds in its open chain, carbonylic form. The role of His143 in the binding of both glucosamine 6-P and reaction intermediates in their extended-chain forms was demonstrated by binding experiments using the reaction intermediate analogue, 2-amino-2-deoxy-D-glucitol 6-phosphate. His143 was also shown to be a critical residue for the conformational coupling between active and allosteric sites. From the pH dependence of the reactivity of the active site histidine to diethyl dicarbonate, we observed a pK_a change of 1.2 units to the acid side when the enzyme undergoes the allosteric T to R transition during which the side chain of Glu148 moves toward the active site. The kinetic study of the Glu148-Gln mutant deaminase shows that the loss of the carboxy group and its replacement with the corresponding amide modifies the k_{cat} versus pH profile of the enzyme, suggesting that the catalytic step requiring the participation of His143 has become rate-limiting. This, in turn, indicates that the interaction Glu148-His143 in the wild-type enzyme in the R state contributes to make the enzyme functional over a wide pH range.

The enzyme glucosamine-6-phosphate deaminase (EC 3.5.99.6, formerly glucosamine 6-phosphate isomerase, EC 5.3.1.10) from *Escherichia coli*, catalyzes the reversible conversion of D-glucosamine 6-phosphate (GlcN6P)[1] into D-fructose 6-phosphate (Fru6P) and ammonia (*1*, *2*). It shows an absolute specificity for the α-anomer of GlcN6P (*2*), and its reaction mechanism involves a ring-opening step, followed by an enolization step that proceeds through a *cis*-enolamine (2-amino-2-deoxy-D-*arabino*-hex-2-enitol 6-phosphate) and its tautomeric imine (2-deoxy-2-imino-D-*arabino*-hexitol 6-phosphate) as reaction intermediates (*2*). This mechanism is similar to that of other ketose-aldose isomerases (*2*, *3*), and it is illustrated in Figure 1, which also summarizes the main results of this research. The enzyme from *E. coli* is the most studied GlcN6P deaminase, and it has been structurally (*4*, *5*) and functionally characterized (*6*−*8*). It is an allosteric enzyme activated by *N*-acetylglucosamine 6-phosphate (GlcNAc6P), and its allosteric kinetics can be well accounted for by the Monod-Wyman-Changeux (MWC) model (*9*, as shown by Altamirano et al., *7*). Like most allosteric enzymes, it is a *K*-system, i.e., regulation is the result of a change in the apparent affinity of the enzyme caused by the allosteric transition, without any change in the catalytic constant, k_{cat}. Structural models of the enzyme in its R [PDB 1dea, 1hor, 1hot, (*4*)] and T allosteric states [PDB 1cd5, (*5*)] were obtained. The crystallographic structure of the enzyme in its R-state complexed to the dead-end

† This research was supported by grants from the National Autonomous University of Mexico (UNAM) DGAPA-UNAM IN201295 and from The National Council of Science and Technology CONACYT (México), project 25258-N. G.M.M. was the recipient of a Ph.D. student fellowship from CONACYT, Mexico.

* Address correspondence to this author: email calcagno@bq.unam.mx; fax + (52) 5616 2419,

‡ Universidad Nacional Autónoma de México, Mexico City, DF, Mexico.

§ Institut de Biologie Physico-Chimique, Paris, France.

[1] Abbreviations: GlcN6P, glucosamine 6-phosphate; GlcNAc6P, *N*-acetyl- glucosamine-6-phosphate; GlcN-ol-6P, 2-amino-2-deoxy-D-glucitol 6-phosphate; DEDC, diethyl dicarbonate.

10.1021/bi0105835 CCC: $20.00
Published on Web 08/03/2001

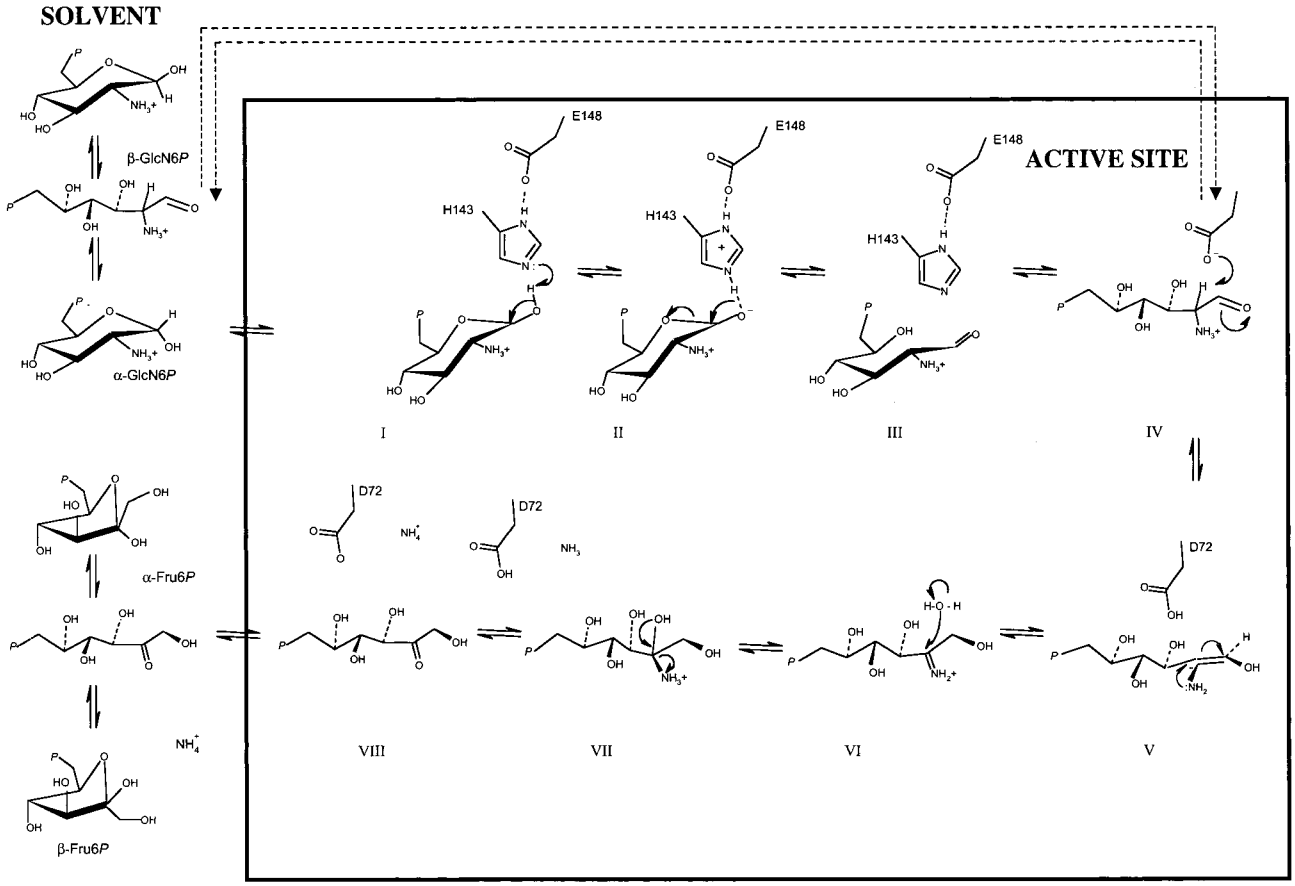

FIGURE 1: Scheme of the chemical mechanism of the reaction catalyzed by *E. coli* GlcN6P deaminase, which resumes data from previous research (*2*, *4*) and the results of the present paper. The dotted arrows correspond to the equilibrium of the enzyme with *aldehydo*-GlcN6P. The contribution of this form of the substrate to the reaction rate is discussed in the text.

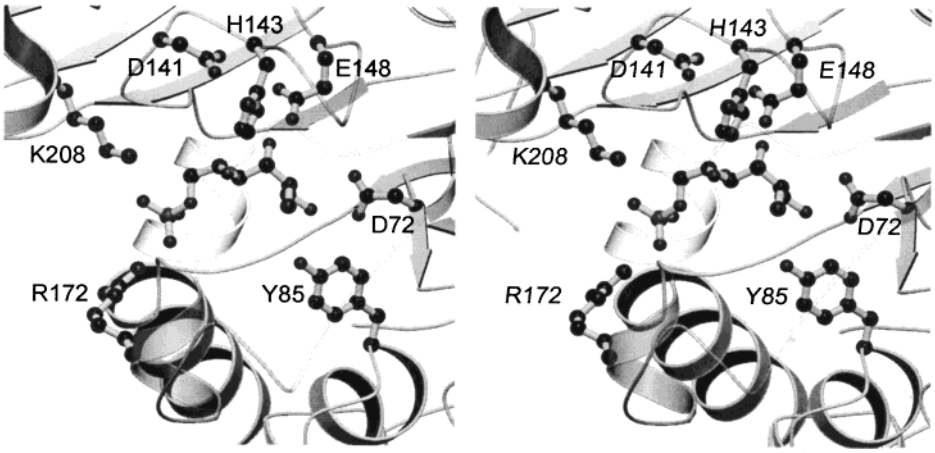

FIGURE 2: Stereo drawing showing the active site of *E. coli* GlcN6P deaminase in the R allosteric state. A molecule of GlcN-ol-6P, a dead-end inhibitor of the enzyme, appears bound to the site, and the side chains of the functionally significant residues discussed in the text, are depicted using stick and ball representation. This figure was generated from the coordinates of the deaminase-GlcN-ol-6P complex (PDB 1hor), using the graphics program MolScript (*38*) compiled for Linux and rendered to the present version with Raster-3D (*39*).

inhibitor 2-amino-2-deoxy-D-glucitol 6-phosphate (GlcN-ol-6P) (PDB 1hor) allowed the precise identification of the catalytic pocket (Figures 2 and 3). The enzyme is a hexamer of identical subunits, arranged as a dimer of trimers. The comparison of the structure of the hexamer in the R and T conformations provided a first geometrical description of the allosteric transition. This consists of a concerted change in the quaternary structure, as predicted by the MWC model (*9*), accompanied by well-defined internal rearrangements in each monomer (*5*). The catalytic mechanism of GlcN6P deaminase, as originally proposed by Midelfort and Rose (*2*), has been reexamined in the light of the crystallographic structure (*4*). Using the three-dimensional structure of the enzyme complexed with GlcN-ol-6P as well as the modeled complex of the enzyme bound to α-D-pyranosyl-GlcN6P, it was possible to propose some functional roles for several active-site residues (*4*). The complex of the enzyme with the inhibitor GlcN-ol-6*P* (PDB 1hor) shows the ligand in an almost extended conformation. This conformation should be similar to that adopted by the bound *aldehydo*-GlcN6P. The proximity of the carboxylate group of Asp72 to the C1−C2 bond of GlcN-ol-6P suggests that this acid residue is the

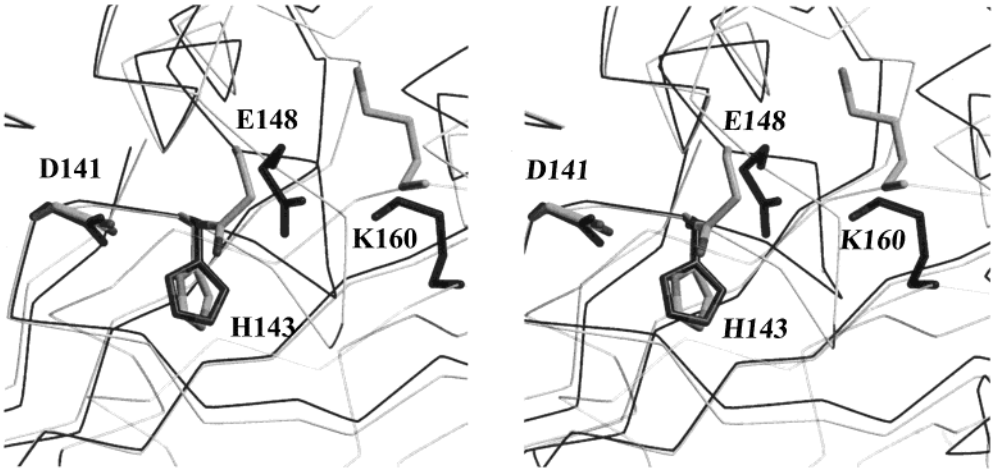

FIGURE 3: Stereopair showing the displacement of the side chain of Glu148 in the allosteric transition of *E. coli* GlcN6P deaminase. Its carboxylate group appears at interaction distance with the Nδ1 atom of His143 when the enzyme is in the R allosteric state (gray; Nδ1-(His143)-Oϵ2(Glu148) distance = 2.71 Å) and moves toward the allosteric site where it forms a salt bridge with the ammonium group of Lys160 (black). The interaction Asp141-His143 is conserved in both conformational states; the corresponding distances are Nδ1(His143)-Oδ2(Asp141) = 3.33 Å (R form) and Nδ1(His143)-Oδ2(Asp141) = 2.6 Å (T form). This image was generated from the coordinates of the deaminase with the active site occupied by GlcN-ol-6P (PDB 1hor) and from those for the ligand-free structure (PDB 1cd5), as described in Figure 2. Overlapping of both set of coordinates was performed with the program Swiss-PdbViewer (*41*).

general-base catalyzing the GlcN6P enolization by abstraction of the C-2 proton. Indeed, its replacement by asparagine decreased the k_{cat} for the forward reaction by 4 orders of magnitude (S. Lara-González, unpublished). The O5 in the inhibitor molecule corresponds to O5 of the open-chain substrate and becomes the pyranose oxygen in the cyclic form of the sugar. This atom contacts with Nϵ2 of His143, suggesting that this histidine residue could play a role in the ring opening of α-D-GlcN6*P* (*4*). The imidazolic Nδ1 of His143 side-chain appears hydrogen-bonded to the carboxylates of Asp141 and Glu148 when the enzyme is in the R allosteric conformation. This arrangement changes when the enzyme goes from the R to the T allosteric state. A local displacement of the loop 144−154 occurs, resulting in a reorientation of the side chain of Glu148, which moves toward the allosteric site and forms a salt bridge with the side chain of Lys160 (Figure 3). This lysine residue is part of the allosteric site and contributes to the binding of the phospho group of GlcNAc6P. This is the most conspicuous tertiary structural change produced by the R−T transition in the deaminase monomer, and it occurs independently of the quaternary structural change, which consists of an overall rotation of the enzyme subunits (*5*). One of the consequences of the local structural change is that the triad Asp141-His143-Glu148, present in the R state, becomes the dyad Asp141-His143 in the T-state (Figure 3). The arrangement around His143 in the active site of GlcN6P deaminase resembles the active site of serine proteases. In both cases, the Nδ1 atom of the active-site histidine makes contact with an activating carboxy group, while the Nϵ2 is able to transfer a proton, after being transitorily protonated during the catalytic cycle (*4*). In the R state of GlcN6P deaminase, which is the conformation expected to be responsible for most of its catalytic activity, there are two carboxy groups simultaneously interacting with the Nδ1 atom from His143. The importance of this triadic arrangement around His143 can be inferred from the sequence alignment shown in Figure 4. In those deaminases known to be allosteric, the triad Asp141-His143-Glu148 is absolutely conserved (Figure 4A). Histidine-aspartate pairs are common in the active site

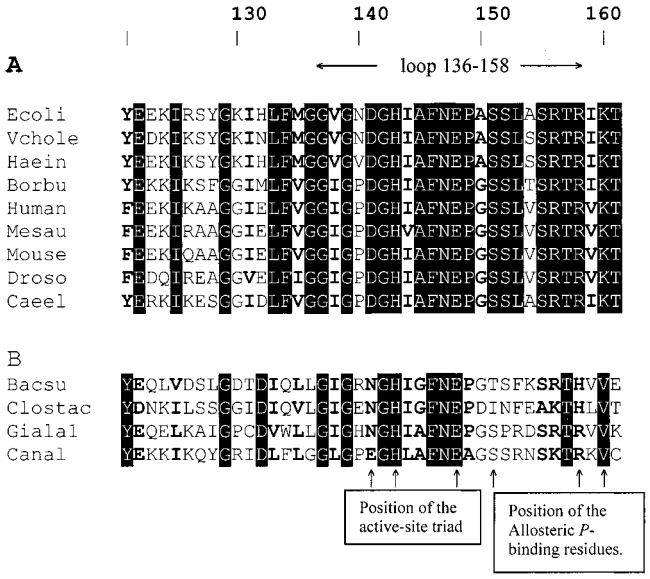

FIGURE 4: Alignment of several orthologous sequences of GlcN6*P* deaminases from bacteria and eukaryota. *Escherichia coli*, (Ecoli); *Vibrio cholerœ*, (Vchole); *Hœmophillus influenzœ*, (Haein); *Borrelia burgdorferi*, (Borbu); *Homo sapiens*, (Human); *Mesocricœtus auratus* (Mesau); *Mus musculus* (Mouse); *Drosophila melanogaster*, (Droso); C*œnorabditis elegans*, (Caeel); *Candida albicans*, (Canal); *Bacillus subtilis*, (Bacsu); *Clostridium aceticum*, (*Clostac*)*; Giardia lamblia*, gene 1 (Giala1). (A) The orthologous group of GlcN6*P* deaminases known to be allosteric (*E. coli*, mammals, *Drosophila*) or predicted to be; all have the residues involved in binding the allosteric phosphate. These allosteric functional residues are Arg158, Lys160, Ser151, as well as Thr161 and Tyr254 (*40*), not shown here. In this group, the triad 141−143−148 is invariant. (B) Deaminases known to be nonallosteric (*Giardia*, *Candida*) or those lacking the signature for the binding site for the allosteric phosphate (Gram positive bacteria). Sequences were obtained from GeneBank (http://www.ncbi.nlm.nih.gov/genbank) and TIGR (http://www.tigr.org) databases. Identical amino acids within each subset are shown on a black background while similarities appear in bold characters. The segment 136−158 in *E. coli* deaminase is a loop connecting the sixth and the seventh β-strands (E and C′ strands in ref 4). The position of the active-site triad and the phospho group binding residues in the allosteric site are indicated with arrows. This alignment was produced with the program Multalin 5.4.1 (*42*).

of many enzymes; they are present in the famed catalytic triad in serine-proteases (*10*) and in other enzymes such as D-glucarate dehydratase (*11*), L-lactate dehydrogenase (flavocytochrome b_2) (*12*), and several hydrolytic enzymes (*13*).

A ring-opening mechanism of cyclic sugar substrates using a histidine imidazole as a general acid or base catalyst has been proposed for those aldose-ketose isomerases which contain a histidine-carboxylic amino acid pair, such as phosphoglucose isomerase (*14*), GlcN6P synthase (Fru6P-glutamine amidotransferase) (*15*), L-arabinose isomerase (*16*), and D-xylose (D-glucose) isomerase. However, in the last enzyme the catalytic role of the active-site histidine in sugar ring-opening, based on the crystallographic structure (*17*), was not supported by site-directed mutagenesis experiments (*18*).

The purpose of this research is to characterize the functional role of His143 and the carboxylic residues which contact it in *E. coli* GlcN6P deaminase and to correlate their structural changes with the allosteric properties of the enzyme. For this, we have used a combined approach of site-directed mutagenesis and chemical modification. Our results demonstrate that His143 and its flanking carboxylic residues have multiple roles in the catalytic and allosteric properties of GlcN6P deaminase.

MATERIALS AND METHODS

Biochemicals. Diethyl dicarbonate, $(EtO\text{-}CO\text{-})_2O$ (DEDC), also called diethyl pyrocarbonate (DEPC), and most biochemicals were purchased from Sigma-Aldrich Química S. A. de C. V. (Toluca, Edo. Mex., Mexico). *N*-6-aminohexanoylglucosamine-6-P agarose, GlcNAc6P, GlcN-ol-6P, ^{14}C-labeled GlcNAc6P and ^{3}H-labeled GlcN-ol-6P, were all prepared as previously described (*7*). The oxime of Fru6P (2-(hydroxyimino)-2-deoxy-D-*arabino*-hexitol 6-phosphate) was prepared from Fru6P according to Finch and Merchant (*19*). 2,5 *anhydro*-D-mannitol 6-P was prepared from the corresponding nonphosphorylated compound (Sigma-Aldrich) by phosphorylation with 1.2 molar excess of $MgATP^{2-}$ and yeast hexokinase (Sigma H5625, 2.5 U mL^{-1}). The product was passed through a column packed with Dowex 50 H^+ equilibrated and eluted with water. Then, 2,5 *anhydro*-D-mannitol 6-P was purified on DEAE cellulose (Whatman), packed in 100 mM pyridine: 1 M formic acid and eluted with the same buffer. The *O*-methyl glycosides of Fru6P (mixed α and β glycosides) were prepared by methylation of Fru6P, according to Fishbein et al. (*20*). Phosphate esters were detected and quantified according to Ben-Yoseph et al. (*21*). All other chemical reagents were of suitable grade and purity for their immediate use.

Bacterial Strains and Mutagenesis. Site-directed mutations were constructed by the technique of oligonucleotide-directed mutagenesis, using the Kunkel method, as described by Sambrook et al. (*22*) with the *nagB* gene inserted in the single-strand vector pTZ18R. The single mutations created were His143 (CAT) to Gln(CAA), Asp141 (GAC) to Asn (AAC), and Glu (GAA to Gln(CAA)). The replacement of each carboxylic amino acid for its corresponding amide was chosen as the most conservative mutation, changing the pH-dependent electrostatic properties of the active site but maintaining the side chain polarity in order to minimize any active site distortion. Phagemids, pTZ(NagB), carrying the mutations were verified by sequencing and were used to transform the Δ*nag* strain IBPC590 (*23*). This strain is Δ*lacI* and expresses the deaminase constitutively from the plasmid *lac* promoter. Details of the procedure and a more complete description of the bacterial strain were already reported (*7*).

Enzyme Purification and Assays. Wild-type GlcN6P deaminase and the mutants used in this research were all purified by allosteric affinity chromatography, as previously reported (*6*, *8*). The purity of the enzymes was verified by SDS−PAGE. These mutations are not expected to produce a significant change of the molar absorptivity of the enzyme, and thus, the value for the wild-type enzyme (20.0×10^4 M^{-1} cm^{-1}) was used to calculate the molar concentration of these mutant forms. GlcN6P deaminase assays and analyses of kinetic data were performed as previously reported (*6*, *7*). Rate measurements were made at pH 7.7, at 30 °C in 50 mM Tris-HCl buffer, unless otherwise indicated. When kinetic parameters were measured as a function of pH, the ternary ACES-Tris-ethanolamine buffer was used to keep ionic strength variations at a minimum (*24*). The measurement of the reverse reaction rate was performed in an incubation mixture prepared in the same buffer and containing variable concentrations of Fru6P and NH_4HCO_3. The GlcN6P formed was measured at fixed times, using a modified Morgan-Elson procedure, as already described (*6*).

Measurement of the Dissociation Constant of the Allosteric Activator. The dissociation constant for GlcNAc6P and GlcN-ol-6P was determined by ultracentrifugation according to the procedure of Howlett (*25*) as modified by Montero-Morán et al. (*8*).

Chemical Modification by DEDC of the Wild-Type and Mutant GlcN6P Deaminases. Kinetic Analysis of its pH-Dependence. Diethyl dicarbonate shows a good specificity for the carboxyethylation of histidine residues near neutral pH (*26*), but it is unstable in aqueous media; its decomposition rate depends on temperature, pH and buffer composition (*27*). Solutions of approximately 50 mM DEDC in cold absolute ethanol were prepared immediately prior to use. The exact DEDC concentration was calculated by means of its reaction with imidazole, using the known molar absorptivity for *N*-carboxyethylhistidine ($\epsilon_{230} = 3.0 \times 10^3$ M^{-1} cm^{-1}, *27*).

Carboxyethylation of GlcN6P deaminase was carried out by incubating the protein (1−5 μM) with DEDC in 0.2 M HEPES buffer at variable pH. The final ethanol concentration in the reaction mixture never exceeded 5%. The reaction was brought to a halt by the addition of histidine, to obtain a final concentration of 1 mM. Then, a series of rate measurements at variable GlcN6P concentrations were run, to determine the kinetic parameters of the enzyme. Despite the great molar excess of DEDC over the enzyme, pseudo-first-order kinetics were never attained because of the instability of the reagent in aqueous solution. To correct the kinetic data to allow for hydrolysis of DEDC, the pseudo-first-order rate-constants for this side reaction were determined through the pH range explored. These data were used to correct the reaction rates of deaminase modification, according to Gomi and Fujioka (*28*).

RESULTS

The Replacement His143-Gln Drastically Impairs the Activity of the Enzyme in the Forward but not in the Backward Direction of the Reaction. The curves of initial

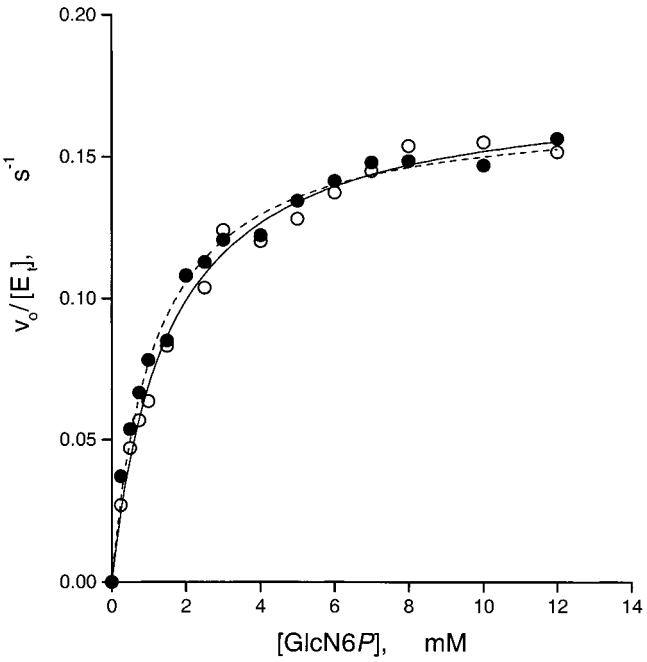

FIGURE 5: Initial velocities versus substrate concentration curves for the His143-Gln mutant form of GlcN6P deaminase. Data were obtained in the absence (broken line, ○) or in the presence (solid line, ●) of 2 mM GlcNAc6P. Assays were performed using mutant GlcN6P deaminase (0.2 μM) in a final volume of 200 μL in 50 mM Tris-HCl buffer (pH 7.7) at 30 °C, as described (*7*). Data were fitted to the hyperbola. The fitted kinetic parameters are shown in Table 1B.

velocities versus GlcN6P concentration for His143-Gln deaminase in the forward direction of the reaction are hyperbolic. This result contrasts with the kinetic behavior of the wild-type enzyme, which displays strong homotropic cooperativity (*6*). The addition of a saturating concentration of GlcNAc6P did not produce significant changes in its kinetic parameters (Figure 5 and Table 1B). The mutation produces a remarkable loss of activity; the corresponding k_{cat} is 3 orders of magnitude lower than the value for the wild-type protein, while the corresponding K_m for GlcN6P shows only a small increase (less than 2-fold) compared to the allosterically activated wild-type enzyme. In agreement with the loss of homotropic cooperativity, GlcN-ol-6P, which acts as a dead-end inhibitor by binding at the active site, binds hyperbolically to this mutant enzyme. The corresponding K_d, determined by direct binding, is 17 times higher than the value for the wild-type enzyme (Table 1A). This mutant form, although it is much less active than the wild-type, behaves kinetically as if it were locked in a conformation similar to the R state of the wild-type enzyme, displaying a K_m value for GlcN6P that is close to that for the wild-type enzyme, either in the presence or the absence of the allosteric activator (Figure 5 and Table 1B). Although there is no substrate homotropic cooperativity, some cooperativity is observed in the GlcNAc6P binding curves. The $[GlcNAc6P]_{0.5}$ values for the wild-type enzyme and the mutant are the same (Table 1A).

Substrate homotropic cooperativity is also absent in the His143-Gln mutant enzyme when studied in the reverse direction of the reaction. Plots of velocity against substrate concentration show substrate inhibition by ammonium ion and even by Fru6P, at high concentrations. To determine the k_{cat} value for the reverse reaction, we performed the kinetic measurements out of the inhibitory range (Figure 6). Data were fitted to the following equation:

$$v_0 = [k_{cat}[E_t][NH_4^+][Fru6P]]/[K_m^{[NH_4^+]}K_m^{[Fru6P]} + K_m^{[Fru6P]}[NH_4^+] + K_m^{[NH_4^+]}[Fru6P] + [NH_4^+][Fru6P]] \quad (1)$$

The kinetic parameters obtained are shown in Table 1C. The fitted k_{cat} value for the reverse reaction catalyzed by the His143-Gln mutant, is 10.3 s^{-1}, which is close to the value for the wild-type enzyme (15.2 s^{-1}). This contrasts with the decrease of 3 orders of magnitude in the k_{cat} for the forward reaction (Table 1B).

Inhibition by Analogues of Fru6P. To know more about the form of Fru6P interacting with the active site of the enzyme, we tested the following Fru6P analogues as potential GlcN6P deaminase inhibitors in the forward direction of the reaction (Figure 7): (I) 2,5 *anhydro*-D-mannitol 6-P, which is structurally similar to the β-anomer of furanose-Fru6P, the most abundant Fru6P anomer in solution (*29*); (II) The *O*-methyl glycosides of Fru6P (mixed α- and β-isomers) which are structurally related to the corresponding anomers of furanose-Fru6P; (III) The oxime of Fru6P, (2-hydroxyimino)-2-deoxy-D-*arabino*-hexitol 6-phosphate, which can be considered as an analogue of the open-chain form of this substrate. Its structure is also closely related to 2-deoxy-2-imino-D-*arabino*-hexitol 6-phosphate, a postulated reaction intermediate (VI in Figure 1). Oximes are formed in either Z or E isomers, but E forms are predominant (*30*). The kinetic study of the wild-type GlcN6P deaminase, in the presence of these compounds gave the inhibition constants shown in Figure 7.

pK_a of the Active Site Histidine and Its Modification by the Allosteric Transition. GlcN6*P* deaminase largely exists in the T conformation and it crystallizes in this state in the absence of ligands (*5*). This is reflected in the high value for the allosteric constant ($L = 10^4$) for the wild-type enzyme (*7*, *8*). The allosteric equilibrium is shifted to the R state by saturation with the allosteric activator, which binds exclusively to the R form (*7*). Taking advantage of this fact, we could analyze the pH-dependence of the reaction rate of GlcN6P deaminase with DEDC, when the enzyme is in either allosteric state. The treatment of the wild-type deaminase with this reagent results in its complete inactivation. When data were corrected for DEDC hydrolysis (*28*), pseudo-first-order kinetics were always obtained. The number of chemically modified histidine residues was determined spectrophotometrically; 4.9 residues per chain were ethoxycarbonylated at pH 8.0 with a second-order rate-constant of 1.40 $\pm$ 0.3 M^{-1} s^{-1}.

Saturation with the competitive inhibitor, GlcN-ol-6P, completely protects the enzyme activity against DEDC inactivation. On the other hand, displacing the allosteric equilibrium toward the R state by saturation with GlcNAc6P, produces a partial protection (Figure 8). This is evidence for the heterotropic conformational change at the active site and shows that the empty active site in the R state is not closed and inaccessible to DEDC.

The spectrophotometric assay measures 3.6 residues modified by DEDC per chain in the GlcN-ol-6P protected GlcN6P deaminase. This modified enzyme displays similar kinetic

Table 1: Kinetic and Binding Properties of the Mutant Form His143-Gln of *E. coli* GlcN6P Deaminase As Compared with Those for the Wild-Type Enzyme[a]

A. Binding Constants

	GlcNAc6*P* binding		GlcN-ol-6*P* binding
	$[GlcNAc6P]_{0.5}$ (μM)	Hill number	K_d (μM)
wild-type	180 ± 50	2.41 ± 0.05	2.23 ± 0.18
His143-Gln	179 ± 32	1.42 ± 0.05	37.7 ± 0.3[b]

B. Kinetic Constants for the Forward Reaction

	without allosteric activator			plus 2 mM GlcNAc6*P*		
	k_{cat} (s^{-1})	$[S]_{0.5}$ or K_m (mM)	Hill number	k_{cat} (s^{-1})	K_m (mM)	Hill number
wild-type[c]	155 ± 7	5.5 ± 0.2	2.9 ± 0.1	158 ± 8	0.75 ± 0.05[d]	2.5 ± 0.2
His143-Gln	0.18 ± 0.07	1.18 ± 0.02	1.01 ± 0.04	0.17 ± 0.08	1.17 ± 0.04	1.05 ± 0.07

C. Kinetic Constants for the Backward Reaction

	K_m^{Fru6P} (mM)	$K_m^{NH_4^+}$ (mM)	k_{cat} (s^{-1})	Hill number
wild-type[c]	0.9 ± 0.1	18.0 ± 4.0	15.2 ± 0.8	1.6 ± 0. 05
His143-Gln	0.15 ± 0.02	0.10 ± 0.009	10.3 ± 0.08	1.02 ± 0.01

[a] Measurements were made at pH 7.7 and 30 °C. Data were fitted by nonlinear regression analysis to hyperbolae, to the Hill equation (from data around $S_{0.5}$ value), or to the MWC equation (*9*). [b] The corresponding K_i for GlcN-ol-6P as a competitive inhibitor is a close value to this, 49.5 ± 1.2 μM. [c] Data for the wild-type GlcN6P deaminase were taken from ref *40* for the forward reaction and from new experiments for the reverse reaction. K_m and k_{cat} values for the wild-type enzyme in ref *6* (forward and backward reaction) correspond to the GlcN6P deaminase prepared from the chromosomal copy of *E. coli* B strain (ATCC 11303) and are different from the present values obtained for the overproducing strain in which the cloned *nagB* gene is derived from the K12 strain. [d] Data were also fitted to the MWC equation (*9*); a K_R value of 0.98 ± 0.08 mM was obtained, which is close to the corresponding K_mGlcN6P value for the activator-saturated enzyme.

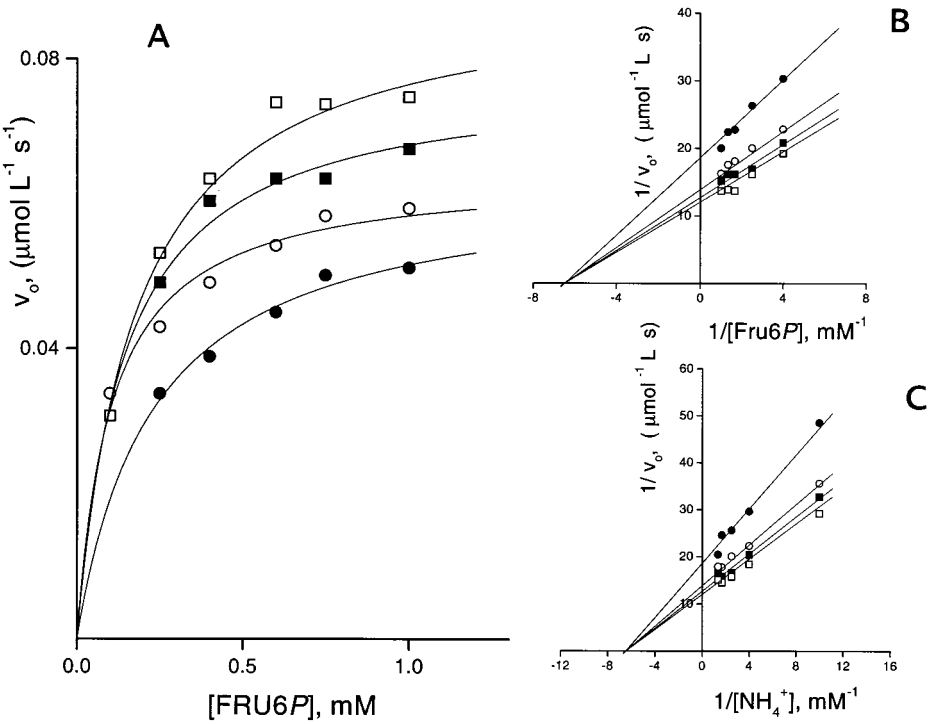

FIGURE 6: Kinetic study of the reverse reaction catalyzed by His143-Gln deaminase. (A) Initial velocities versus Fru6P concentration at different fixed concentrations of ammonium ion. In the explored concentration range, substrate inhibition by NH_4^+ can be considered negligible. Data were fitted to eq 1 and are shown in Table 1C. Insets B and C show the corresponding double reciprocal plot for the same data. For panels A and B, the ammonium concentrations were (●) 0.1 mM; (○) 0.25 mM; (■) 0.4 mM; (□) 0.6 mM. In the inset C, Fru6P concentrations and their corresponding symbols were the same. These experiments were performed in the presence of 0.2 mM GlcNAc6P.

parameters and the same allosteric activation pattern as the wild-type protein. This implies that the residue whose chemical modification inactivates the enzyme and which is protected by saturation with GlcN-ol-6P should be located at or near the active site. This is His143 because it is the only histidine present in the active site. This result also proves that the other four modified residues are irrelevant for enzyme function.

The pK_a of the essential histidine residue was calculated from the effect of pH on the rate of modification by DEDC. The apparent pseudo-first-order rate-constant of the reaction with DEDC decreases with H^+ ion concentration, but the curve is not asymptotic to the abscissa and the k_{app} presents a finite value at saturating $[H^+]$. Calling k_1 the pseudo-first-order rate constant independent of $[H^+]$, K_a the dissociation constant of the group whose protonation causes the change

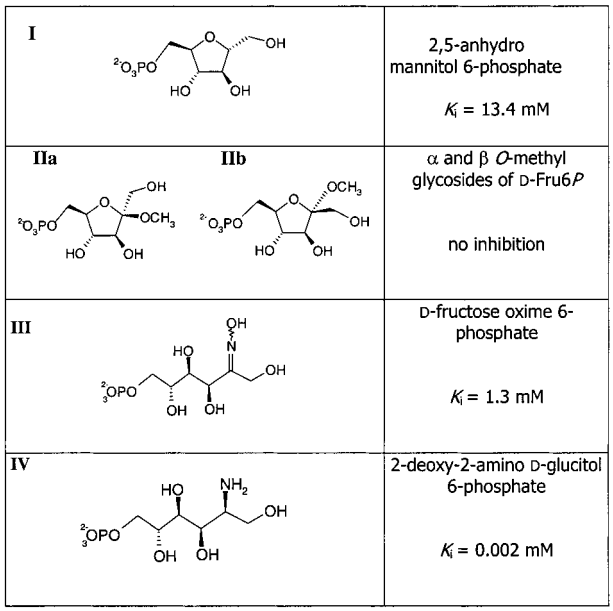

FIGURE 7: Some structural analogues of Fru6P that were tested as inhibitors of GlcN6P deaminase. I and III behave as weak competitive inhibitors with respect to GlcN6P, while IV is a strong inhibitor and probably corresponds to a transition state analogue. The corresponding K_i values are given.

in k_{app} and k_2 the limit value for k_{app} at infinite $[H^+]$, we can write the following expression for the pH dependence of the pseudo-first-order rate-constant:

$$k_{app} = (k_1K_a + k_2[H^+])/(K_a + [H^+]) \qquad (2)$$

It is at first sight surprising that protonation of the histidine does not completely stop its acylation by DEDC, because it depends on the nucleophilic attack of the histidine residue on a carbonyl group of the reagent. Nevertheless, it is possible that a nearby base, e.g., a carboxylate group, may remove H^+ from it. Thus, the reactive species could be the carboxylate-imidazole pair $-COO^-\cdots Im-$. This pair could be protonated with the observed molecular pK_a, to form the equilibrium mixture of $COOH\cdots Im- \rightleftharpoons -COO^-\cdots ImH^+-$ which will display a lower rate constant for reaction with DEDC. The pK_a for the further protonation of this system to yield $-COOH\cdots ImH^+-$ may well be too low to observe.

Table 2 summarizes the results of these titration experiments based on DEDC reactivity. The apparent pK_a of this group is 7.6 ± 0.2 when the enzyme is in the T state. A similar pK_a value, which does not change upon GlcNAc6P addition was found for the mutant Glu148-Gln. It should be noted that the wild-type enzyme in the T-state and the Glu148-Gln mutant, both lack the interaction His143-Glu148. On the other hand, the wild-type enzyme in the R state displays a pK_a of 6.4. Similar measurements were performed using the mutant forms Asp141-Asn and Asp141-Asn:Glu148-Gln. The single mutant Asp141-Asn does not change its kinetic properties upon DEDC treatment, while the double mutant Asp141-Asn:Glu148-Gln behaves similarly to Glu148-Gln deaminase, that is, it shows an apparent pK_a of 7.7 that does not change by saturation with GlcNAc6P (Table 2). These data indicate that Glu148 is the residue affecting the reactivity of His143 by changing its pK_a from 7.6 in the T state to 6.4 in the R state.

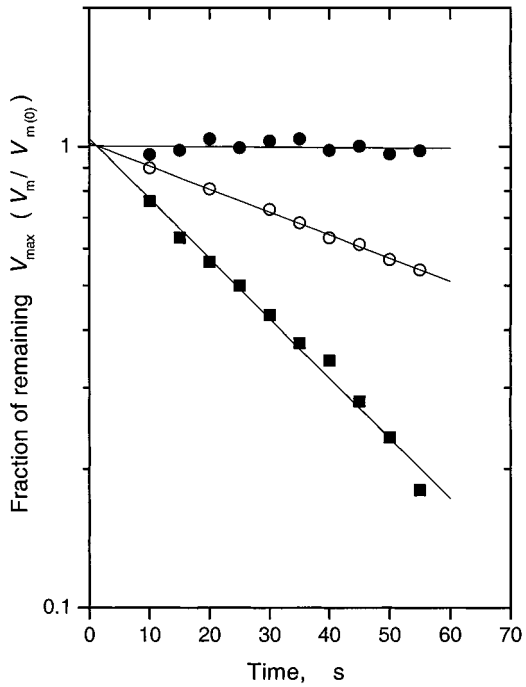

FIGURE 8: Effect of ligands on the inactivation of wild-type GlcN6P deaminase by DEDC. Semilogarithmic plot of the time-course of the fraction of remaining activity of the enzyme. This is defined as the V/V_o ratio, where V_o is the maximal velocity determined in the absence of ligands at zero time. (■) In the absence of any ligand, GlcN6P deaminase is totally inactivated by DEDC. (●) A saturating concentration of the dead-end inhibitor GlcN-ol-6P, fully protected the enzyme. (○) a saturating (2 mM) concentration of the allosteric activator GlcNAc6P slows the inactivation reaction.

Table 2: pK_a Values of the Imidazole Group of the Active Site Histidine (His143), Calculated from the Effect of $[H^+]$ on Its Reactivity toward DEDC

	ligand-free (T state)	with 2 mM GlcNAc6*P* (R state)
wild-type enzyme	7.60 ± 0.2	6.40 ± 0.1
His143-Gln	no change	no change
Glu148-Gln	7.56 ± 0.5	7.63 ± 0.4
Asp141-Asn:Glu148-Gln	7.66 ± 0.58	7.70 ± 0.01
Asp141-Asn	no change	no change

Effect of the Mutations in Residues Asp141 and Glu148 on the pH Curve of the Enzyme. The replacement of either Asp141 or Glu148 by their corresponding amides affects the k_{cat} values similarly. In both cases, they are in the range 6.6−7.8 s^{-1}, that is 40 times higher than the value for the mutant forms involving His143, but 20 times lower than the corresponding k_{cat} for the wild-type enzyme (not shown). Both mutants display substrate inhibition, which was taken into account for data fitting.

The low k_{cat} values of the His143-Gln enzyme were found to be constant over the pH interval 6 to 9. Similarly, the wild-type enzyme does not reveal any protonic equilibrium in the same range (Figure 9A). In contrast, the mutation Glu148-Gln (Figure 9B) and the double mutation Asp141-Asn:Glu148-Gln (not shown) show a decrease of k_{cat} values on the acid side of the range. From the analysis of these data, a pK_a of 6.62 ± 0.04 was obtained. These values did not change in the presence of 2.8 M dimethyl sulfoxide. The Asp141-Asn mutant did not present any apparent pK_a over the same pH range.

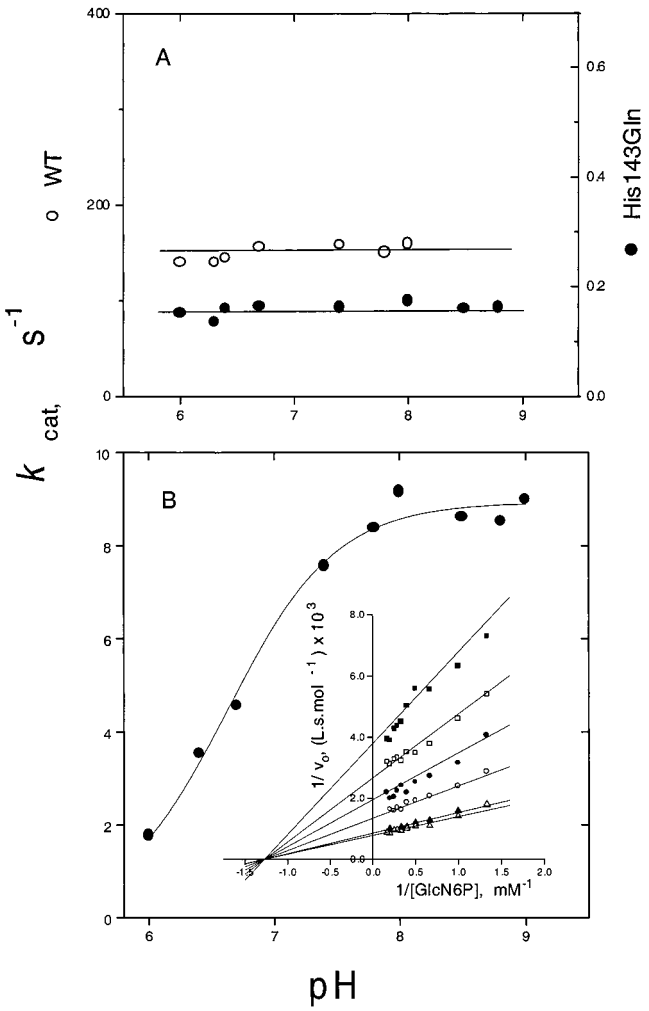

FIGURE 9: (A) k_{cat} versus pH curves for the wild-type deaminase (○) and His143-Gln mutant (●). (B) k_{cat} versus pH curves for Glu146-Gln deaminase. Inset: Double reciprocal plot in which the inhibition pattern by $[H^+]$ is shown. The $[H^+]$ explored were (△) 3.20×10^{-8} M; (▲) 1×10^{-8} M; (○) 6.3×10^{-7} M; (●) 2.5×10^{-7} M; (□) 5.01×10^{-6} M; (■) 2.51×10^{-6} M. Data were fitted to noncompetitive inhibition by nonlinear multiple regression analysis. The fitted value for the involved pK_a is 6.63 ± 0.04 for the Glu148-Gln mutant. The noncompetitive inhibition pattern indicates that this protonic equilibrium affects only the k_{cat} values. In the presence of 20% dimethyl sulfoxide, the pK_a value for Glu148-Gln deaminase remains unchanged (6.63 ± 0.2). Essentially similar results were obtained with the double mutant Asp141-Asn: Glu148-Gln (not shown).

DISCUSSION

The Role of His143 in Functional Coupling of Active and Allosteric Site. The substitution of the catalytic histidine by a glutamine residue produces marked functional changes in GlcN6P deaminase, with respect to the wild-type enzyme. The mutation impairs the enzyme activity and causes the complete loss of the homotropic cooperativity. The mutant enzyme behaves as if it were locked in the R state, displaying hyperbolic kinetics and a K_m value for GlcN6P close to that for the wild-type in the R state (Table 1B). A saturating concentration of GlcNAc6P does not change the kinetics of this mutant deaminase, and both enzymes, wild-type and mutant, bind the allosteric activator with the same affinity (Table 1A). Some degree of cooperativity is present in the GlcNAc6P binding curve of the His143-Gln deaminase, indicating that the allosteric transition is not entirely abolished by the mutation, even if active-site homotropic effects are absent. It is possible that His143-Gln deaminase has a structure close to that of the wild-type R state. A crystallographic study could help to clarify this point. These results emphasize the importance of His143 and the flexible loop containing it, in coupling the local tertiary-structure changes in the active site, to the quaternary concerted transition.

His143 Catalyzes the Ring-Opening of α-D-*GlcN6P but Does not Participate in Ring-Opening of the Furanose Fru6P.* The mutation His143-Gln severely interferes with the catalysis of the deamination reaction, as shown by the decrease of 3 orders of magnitude in the corresponding k_{cat} value. In contrast, the k_{cat} for the reverse reaction is two-thirds the value for the wild-type enzyme (Table 1B), and it is close to the first-order rate-constant for the spontaneous ring-opening of either α- or *β*-D-Fru6P, which is 20 s^{-1} (*29*). The most abundant Fru6P anomer in aqueous solution is α-D-Fru6P (mole fraction 0.81), while the rest is mainly *β*-D-Fru6*P* accompanied by a small concentration of the free carbonylic species (mole fraction, 0.022), which must be the true substrate for the reverse reaction (Figure 1, VIII). From the data in Table 1, we can see that the ratio $V^{forward}/V^{backward}$ changes from 10.2 for the wild-type enzyme to 0.02 for the His143-Gln mutant. Binding of the *aldehydo* form of GlcN6*P* (Figure 1, IV), which is present in a small concentration at equilibrium, should easily occur (dotted arrows in Figure 1). The enzyme recognizes the open-chain analogues of the substrate, and it is expected that it also easily binds the open form of the substrate. After the rapid exhaustion of this species, the spontaneous ring-opening in the solution, which is very low (*2*), becomes the rate-limiting step for the catalyzed forward reaction. Therefore, the contribution of *aldehydo*-GlcN6*P* to the rate of the forward reaction is negligible and uncatalyzed ring-opening does not contribute to the measured reaction rate. On the other hand, the absence of the *aldehydo*-GlcN6P cyclization step does not affect the rate of the reverse reaction, indicating that the open-chain GlcN6P can diffuse to the solution, where it slowly forms the pyranose sugar (Figure 1).

Additional evidence supporting the hypothesis that the enzyme binds or releases the open carbonylic form of Fru6P, comes from inhibition experiments by Fru6P analogues (Figure 7). 2,5-*Anhydro*-D-mannitol 6-P, a close analogue of *β*-D-Fru6P, is a low-affinity competitive inhibitor, and the α- and *β*-*O*-methyl glycosides of Fru6P are not inhibitors at all. On the other hand, the oxime of Fru6P, which is an analogue of its open form, inhibits competitively the enzyme with respect to GlcN6P, with a K_i of 1.7 mM. This oxime is structurally similar to the reaction intermediate 2-deoxy-2-imino-D-*arabino*-hexitol 6-phosphate (VI, Figure 1), which is a tautomer of the corresponding *cis*-enolamine (V). Midelfort and Rose (*2*) had proposed that this imine intermediate is the species adding a water molecule in the reaction. The inhibition by the analogue of intermediate VI supports the presence of this intermediate in the reaction sequence.

It is also worth mentioning that docking experiments on the crystallographic model of the enzyme show that the furanose form of Fru6P built into the active site, presents unfavorable steric interactions with His143 (E. Rudiño-Piñera and E. Horjales, personal communication). It is, after all, rationale that a ring-opening step has evolved only for

GlcN6P, which is the substrate in the physiological direction of the reaction catalyzed by *E. coli* enzyme (*31*).

Differential Binding Properties of His143 also Contribute to Catalysis. The K_d value for the competitive inhibitor, GlcN-ol-6P, determined by direct binding experiments, is 17 times higher for the mutant enzyme than for the wild-type (Table 1A). This suggests that, in addition to its catalytic role as a general base, His143 preferentially binds the extended-chain intermediates of the reaction. This is consistent with the structural data of the deaminase with GlcN-ol-6P bound to its active site, which shows that the O5 atom of the inhibitor is hydrogen-bonded to Nϵ2 from His143 (PDB 1hor). A similar role in binding the extended reaction intermediates is played by Tyr85, whose hydroxyl group appears to be contacting the amino group of GlcN-ol-6P. Its replacement by phenylalanine produces a similar increase in $K_i^{GlcN-ol-6P}$ and $K_d^{GlcN-ol-6P}$, while the enzyme displays a similar K_m^{GlcN6P} as the wild-type enzyme (G. Montero-Morán et al., unpublished data). This indicates that neither Tyr85 nor His143 contribute to α-D-GlcN6*P* binding, but that both are involved in binding of its extended carbonylic form. The calculated contribution of His143, on basis of the ligand binding data, is 5.8 kJ mol^{-1}.

pK_a of His143 and Its Relation to the Allosteric Transition. The Possible Functional Role of Glu148 and Asp141. DEDC is an imidazole-directed reactivity probe, capable of detecting the nucleophilic component in a histidine-carboxylate pair (*26*). According to the crystallographic models of *E. coli* GlcN6P deaminase, the imidazole Nδ1 atom of His143 is at interaction distance with the carboxy oxygen from Asp141 (ligand-free T state, PDB cd5), or contacting the two carboxy groups from both Asp141 and Glu148 (R state, PDB 1hor). In the latter structure, which has its active site occupied by GlcN-ol-6P, the Nϵ atom of His143 is oriented toward the O5 atom of the inhibitor, which can be considered as a model of the extended form of the bound substrate. This arrangement strongly supports the assumption that the predominant tautomer of the imidazole has its δ1N atom protonated (Nδ1H-Im-Nϵ). This tautomer has the electron pair from Nϵ available for nucleophilic catalysis and is the form usually found in the active site of most enzymes containing the aspartate−histidine pair (*31*−*35*).

The group [Nδ1H-Im-Nϵ] is the basic form of a buffer pair and it should react with DEDC producing the *N*-(2-carboxyethyl) derivative on Nϵ. The corresponding protonated and positively charged group is expected to be entirely unreactive. Thus, the variation of the apparent first-order rate-constant for this reaction as a function of pH should give the apparent pK_a value of the modified group. The transition [imidazole]/[imidazolium ion] presents an apparent pK_a of 7.6 when the enzyme is in its T allosteric form and changes to 6.4 in the R state (Table 2). In the T state, the enzyme contains the dyad Asp141-His143 and the observed pK_a probably corresponds to that of His143 imidazole. It is nearly one pH unit higher than the corresponding value for free histidine, as a probable consequence of the interaction of His 143 with Asp141. It is worth noting that the Glu148-Gln mutant, which lacks the possibility of forming the triad, has a pH profile for the reaction with DEDC which is similar to that found for the wild-type enzyme in the T state and that it remains unchanged upon saturation with GlcNAc6P. This underlines the important role of Glu148 carboxylate on His143 reactivity. In addition, the side chain carboxylates of Asp141 and Glu148 may play a structural role, positioning the imidazole ring and favoring the optimal tautomery for catalysis.

*His143 Acts as a Proton Acceptor in the GlcN6*P *Ring-Opening Step.* The kinetic and chemical modification experiments show that protonation interferes with the catalytic role of His143. The role of this residue can be depicted as the abstraction of a proton from the hydroxyl in the anomeric carbon of *pyranose*-GlcN6P by its Nδ atom. The imidazolium group loses then its charge by protonating O5, completing the ring-opening reaction (Figure 1, steps I−III). The structural model of the *E. coli* deaminase bound to the putative transition-state analogue GlcN-ol-6P shows the chain of this competitive inhibitor in an almost completely extended form, with its O5 atom at an interaction distance to Nδ atom of His143. The switching of this hydrogen bond from O1 to O5 implies that the side chain of His143 can occupy two alternative positions, acting as a base in one rotamer and as an acid in the other.

Do Mutations in the Triad Change the pH Curve of the Enzyme? The k_{cat} versus pH curves for the wild-type enzyme and the enzymes with the amino acid replacements Asp141-Asn and His143-Gln do not exhibit any protonic equilibrium in the pH range 6−9. On the other hand, Glu148-Gln deaminase exhibits pK_a of 6.62 ± 0.04 for the change of *V* as a function of pH (Figure 9). This value did not change when the experiment was repeated in the presence of 20% dimethyl sulfoxide (pK_a = 6.63 ± 0.19). These pK_a values correspond to the R state because they derive from experiments with the fully allosterically activated deaminase. The lack of effect of the change in solvent polarity indicates that proton dissociation does not form new charges, which is the case for the imidazolium group of histidine. Furthermore, the absence of any titratable group in similar experiments with the mutant deaminase His143-Gln, supports the attribution of this pK_a to His143. The chemical modification approach allowed the identification of a histidine imidazole with a pK_a = 6.4 in the wild-type enzyme in the R state. It is plausible that in both cases we are detecting the same ionizable group, which does not appear in the k_{cat} versus pH profile of the wild-type enzyme because the catalytic step involved is not rate-limiting. The pK_a value for this group cannot be determined kinetically when the enzyme is in the T form, but the DEDC experiments gave a value that is nearly one pH unit higher than the values from chemical modification and kinetic analysis for the R form. This suggests that Glu148-His143 interaction helps the catalytic function of GlcN6P deaminase by widening the functional pH range of the enzyme in the R state, thus preventing the ring-opening of the substrate from becoming rate-limiting at the acid side of the pH-range. It must be remembered that the R conformer is responsible for most, if not all, the physiological catalytic activity of the enzyme.

Concluding Comments. The present research reveals that His143 plays many functional roles in the active site of GlcN6*P* deaminase from *E. coli.* Site-directed mutagenesis and controlled chemical modification are considered the standard tools for dissecting active or allosteric sites and revealing relations between structure and function. It has been usual to recognize "catalytic" and "binding" residues, but in most cases it is not possible to establish a clear-cut difference between these two categories. Most studies published since the pioneering work on tyrosyl-tRNA syn-

thetase by Fersht et al. (*36*) have shown that this functional dissection is a difficult task because replacement of residues strictly labeled as binding have been shown to cause significant changes in catalytic parameters. This is the case for His143 in *E. coli* GlcN6P deaminase, and the present research shows that this histidine plays multiple roles. It participates in bond breaking and forming in ring-opening of α-D-GlcN6P and also contributes to catalysis by a *differential binding* activity (*37*) in favor of the open-chain and extended reaction intermediates in the subsequent step of the reaction. The present study also implicates His143 and the loop containing it, in the transmission of conformational changes between the active and the allosteric sites. We cannot quantify the contribution of this histidine to site coupling, but the analysis of the structural models shows that this residue is the center of an intricate network of interactions in the R allosteric state, involving the active-site lid and the intersubunit contacts in the allosteric cleft. The loop 136−158 connects the sixth and seventh β-strands in deaminase molecule (*4*). It contains the active-site triad as well as Ser151, one of the residues whose side-chain contributes to bind the phospho-group in the allosteric site. The following short strand (158−161) contains the residues Arg158 and Lys160, which are also part of the phospho-group binding subsite in the allosteric site (Figure 4). It also has Thr161, which forms an intersubunit link in the allosteric site with Tyr254 of the facing subunit in the R state (*8*). His143 contacts one of the Oγ atoms of Glu148 in the R state, whose other Oγ forms hydrogen bonds with the Oβ atoms from Thr166 and Thr163 which are located in the active site lid (segment 162−185) (observation communicated by E. Rudiño-Piñera). In the T state, His143 retains its contact with Asp141, and the displacement of the loop 144−154 puts it in a more open and water-rich environment (*5*). Deciphering this web of multiple interactions to describe cooperative effects in *E. coli* GlcN6P deaminase is a challenging task.

ACKNOWLEDGMENT

The authors gratefully acknowledge Juan-Pablo Pardo and Rosario Muñoz-Clares (National University of Mexico) and also H.B.F. Dixon and Myriam M. Altamirano (Cambridge University, UK) for stimulating and helpful discussions and the critical reading of the manuscript. Enrique Rudiño-Piñera and Eduardo Horjales contributed to this research with fruitful discussions and the communication of unpublished crystallographic results.

REFERENCES

1. Comb, D. G., and Roseman, S. (1958) *J. Biol. Chem. 232*, 807−827.
2. Midelfort, C., and Rose, I. A. (1977) *Biochemistry 16*, 1590−1596.
3. Rose, I. A. (1975) *Adv. Enzymol. 43*, 491−517.
4. Oliva, G., Fontes, M. R. M., Garratt, R. C., Altamirano, M. M., Calcagno, M. L., and Horjales, E. (1995) *Structure 3*, 1323−1332.
5. Horjales, E., Altamirano, M. M, Calcagno, M. L., Garratt R. C., Glaucius O. (1999) *Structure 7*, 527−537.
6. Calcagno, M. L., Campos, P. J., Mulliert, G., and Suástegui, J. (1984) *Biochim. Biophys. Acta 787*, 165−173.
7. Altamirano, M. M., Plumbridge, J. A., Horjales, E., and Calcagno, M. L. (1995) *Biochemistry 34*, 6074−6082.
8. Montero-Morán, G. M., Horjales E., Calcagno, M. L., and Altamirano, M. M. (1998) *Biochemistry 37*, 7844−7849.
9. Monod, J., Wyman, J., and Changeux, J. P. (1965) *J. Mol. Biol. 12*, 88−118.
10. Dodson, G., and Wlodaver, A. (1998) *Trends Biol. Sci. 23*, 347−352.
11. Gulick, A. M., Hubbard, B. K., Gerlt, J. A., and Rayment, I. (2000) *Biochemistry 39*, 4590−602.
12. Gondry, M., and Lederer, F. (1996) *Biochemistry 35*, 8587−94.
13. Quirk, D. J., Park, C., Thompson, J. E., and Raines, R. T. (1998) *Biochemistry 37*, 17958−17964.
14. Malaisse-Lagae, F., Liemans, V., Yayali, B., Sener, A., and Malaisse, W. J. (1989) *Biochim. Biophys. Acta 998*, 118−125.
15. Tepliakov, A., Obmolova, G., Badet-Denisot, M. A., and Badet, B. (1999) *Protein Sci. 8*, 596−602.
16. Banerjee, S., Anderson, F., and Farber, G. K. (1995) *Protein Eng. 8*, 1189−1195.
17. Blow, D. M., Collyer, C. A., Goldberg, J. D., and Smart, O. S. (1992*) Faraday Discuss. 93*, 67−73.
18. Whitaker, R. B., Cho, Y., Cha, J., Carrell, H. L. Glusker, J. P., Karplus P. A., and Batt, C. A. (1995) *J. Biol. Chem. 270*, 22895−22906.
19. Finch, P., and Merchant, Z. (1979) *Carbohydr. Res. 76*, 225−232.
20. Fishbein, R., Benkovic, P. A., Schray, K. J., Siewers, I. J., Steffens, J. J., and Benkovic, S. J. (1974) *J. Biol. Chem. 249*, 6047−6051.
21. Ben-Yoseph, O., Sparkes, M. J.; Dixon, H. B. F. (1993) *Anal. Biochem. 210*, 195−198.
22. Sambrook, J., Fritsch, E. F., and Maniatis, P. (1989) Molecular Cloning, 2nd Ed., Cold Spring Harbor Laboratory Press, Plainview, NY.
23. Plumbridge, J. A. (1992) *J. Gen. Microbiol. 138*, 1011−1017.
24. Ellis, K. J., and Morrison, J. F. (1982) *Methods Enzymol. 87*, 405−426.
25. Howlett, G. J., Yeh, E., and Schachman, H. K. (1978) *Arch. Biochem. Biophys. 190*, 809−819.
26. Miles, E. W. (1977) *Methods Enzymol. 47*, 431−422.
27. Berger, S. L. (1975) *Anal. Biochem. 67*, 428−437.
28. Gomi, T., Fujioka, M. N. (1983) *Biochemistry 22*, 137−143
29. Pierce, J., Serianni, A. S., and Barker, R. (1985) *J. Am. Chem. Soc. 107*, 2448−2456.
30. Bearne, S., and Blouin, C. (2000) *J. Biol. Chem. 275*, 135−140.
31. Vogler, A. P., Trentman, S., Lengeler, J. W. J. (1989) *Bacteriology 171*, 6586−6592.
32. Kossiakoff, A. A., and Spencer, S. A. (1981) *Biochemistry 20*, 6462−74.
33. Bachovchin, W. W. (1985) *Proc. Natl. Acad. Sci. U.S.A. 82*, 7948−51.
34. Bachovchin, W.W. (1986) *Biochemistry 25*, 7751−9.
35. Ash E. L., Sudmeier J. L., De Fabo E. C., and Bachovchin W. W. (1997) *Science 278*, 1128.
36. Fersht, A. R., Shi, J. P., Knill-Jones, J., Lowe, D. M., Wilkinson, A. J., Blow, D. M., Brick, P., Carter, P., Waye, M. M., and Winter, G. (1985) *Nature 314*, 235−238.
37. Albery, W. J., and Knowles, J. R. (1976) *Biochemistry* 15, 5631−5640.
38. Kraulis, P. (1991) *J. Appl. Crystalogr. 24*, 946−950.
39. Merritt, E. A., and Bacon, D. J. (1997) *Methods Enzymol. 277*, 505−524.
40. Lara-González S., Dixon B. F. H., Mendoza-Hernández G., Altamirano M. M., and Calcagno M. L. (2000) *J. Mol. Biol. 301*, 219−228.
41. Guex, N., and Pertsch, M. C. (1997) *Electrophoresis 18*, 2714−2723.
42. Corpet F. (1988) *Nucleic Acids Res. 16*, 10881−10890.

BI0105835